EasyChair Preprint

№ 13594

Thermal- Structural Coupling Characteristic Analysis of Shield Energy Tunnel Under Design Condition

Shouheng Shen, Hui Zhang, Xinru Wang, Yongming Ji and Songtao Hu

June 7, 2024

Thermal- structural coupling characteristic analysis of shield energy tunnel under design condition

Shouheng SHIN[1], Hui ZHANG[1], Xinru WANG[1], Yongming JI[1], Songtao HU[1]

[1] School of Environmental and Municipal Engineering, Qingdao University of Technology, Qingdao Municipality, Shandong Province, China, shinshouheng@163.com

Abstract: With the development of society and the growth of population, the demand for energy continues to increase. Utilizing subway source heat pump technology to extract shallow geothermal energy for cooling or heating for users, making shield tunnel subways become energy tunnels, is one of the most effective technologies to solve the problem of energy demand. However, the thermal impact of heat exchanger operation on tunnel structures still needs further research. Based on COMSOL Multiphysics software, this paper analyzes the heat exchange performance of the Capillary Heat exchanger (CHE) in energy tunnels and the structural mechanical response of shield tunnel segments during CHE operation under typical heating season and cooling season conditions.

The results indicate that the performance of precast CHE in energy tunnels is excellent. A single-ring energy tunnel can provide cooling and heating capacities of 601.62W and 466.28W, respectively, during the cooling and heating seasons, with heat transfer efficiency of 63.46W/m² and 49.19W/m² respectively. The operation of the CHE during the cooling season leads to elongation of the tunnel segments, while during the heating season, compression of the tunnel segments occurs. The maximum tensile stress and maximum compressive stress generated in heating season are 0.60 MPa and 0.73 MPa respectively, while in cooling season they are 0.56 MPa and 0.87 MPa respectively. The compressive stresses generated during the cooling and heating seasons due to CHE operation are far below the compressive limit of C50 concrete, with tensile stresses representing 33% and 23% of the axial tensile strength, respectively.

The calculation results indicate that under the design conditions of the heat pump unit, when the heat exchange between the CHE and the tunnel reaches steady state, the impact of CHE heat exchange on the structural integrity of the shield tunnel is relatively minor.

Keywords: Heat pump, Capillary heat exchanger, Energy tunnel, Thermal-structural coupling

1. INTRODUCTION

According to the data released in the "Annual Development Research Report on Building Energy Conservation in China 2022", in 2020, the energy consumption during the operational phase of buildings in China was 1.06 billion tec (National Bureau of Statistics, 2022), accounting for 21.3% of the total national energy consumption. The carbon emissions were 2.16 billion tons of CO2, approximately 21.7% of the total national carbon emissions (Jiang et al., 2022).

Against this backdrop, the importance of promoting clean energy heating becomes increasingly prominent. Shallow geothermal energy, as a type of clean energy, mainly utilizes the heat energy from the Earth's interior through technologies like heat pumps to achieve centralized heating. Shallow geothermal energy has advantages such as renewability, high efficiency, energy conservation, and environmental friendliness. It not only reduces energy consumption and environmental pollution but also improves heating efficiency and comfort.

The waste heat within subway tunnels, as a form of shallow geothermal energy, has also received widespread attention. Academician Qihu QIAN, a member of the Chinese Academy of Sciences, recipient of the highest international science and technology award, and professor at the Army Engineering University, clearly stated at the "Geothermal Energy Development and Utilization with Earth Energy Storage Systems" seminar: "We should strengthen research and utilization efforts on 'tunnel energy' to turn waste heat in tunnels into sources for heating and cooling" (Geothermal energy information, 2023).

Laying the heat exchange pipeline in underground continuous walls, building foundation piles, and tunnel linings, and utilizing geothermal heat pump technology to extract shallow geothermal energy, allows the building's foundation components to become part of an underground energy structure. Among these, the underground energy structure based on tunnels as foundation components is referred to as an energy tunnel.

Brandl (2006; 2016) conducted on-site experiments in the Lainz Tunnel in Austria, testing its heat exchange capacity. Through geothermal heat pump technology, they used energy piles buried in the tunnel as front-end heat exchangers to provide heating or cooling for a nearby school, further exploring the economic feasibility and viability of installing heat exchangers in tunnels. Adam and Markiewicz (2009) proposed an innovative construction method where they placed the ground heat exchanger pipes in geotextile fabric, referred to as "energy geotextile." This technique enables the prefabricated construction of tunnel linings and ground heat exchangers. By employing this construction method, not only can the waterproofing performance of tunnel linings be ensured, but also protection for the heat exchange pipeline can be provided, thus enhancing construction efficiency. To further reduce the difficulty of laying heat exchange pipes and their impact on tunnel structures, the team led by Songtao HU at Qingdao University of Science and Technology proposed laying capillary heat exchangers (CHE) in the lining of subway tunnels, as front-end heat exchangers for ground heat pump systems (Wang et al, 2013). The capillary front-end heat exchanger extracts waste heat generated by various equipment in the subway tunnel to provide heating for users, thus this ground heat pump system is referred to as a subway source heat pump system (SSHPS). These capillary heat exchangers have advantages such as simple construction method, small footprint, large heat exchange area, uniform heat exchange, high overall heat transfer coefficient, flexible layout, and easy integration with subway tunnel structures. The applicability, heat exchange performance, and design parameters of capillary heat exchangers in mining method tunnels have been validated through scaling experiments, numerical simulations, and demonstration projects.

Currently, shield tunnel, due to its relatively high technical and economic feasibility, is increasingly serving urban construction in China. Combining capillary heat exchangers (CHE) with shield tunnel segments as front-end heat exchangers for subway source heat pumps is referred to as shield tunnel energy segments. This can make a significant contribution to urban energy conservation, emissions reduction, and sustainable development. However, the service life of urban tunnels is typically around 100 years, and the thermal stresses generated by the operation of heat exchangers should not be ignored. Xia et al. (2014) established a thermal-structural coupling finite element model for energy tunnels and studied the mutual influence between heat exchangers installed in tunnels and tunnel structures in cold regions. Zhu (2020) analyzed the maintenance process, construction process, as well as stress and strain changes in tunnel segments during the heat exchange process based on the energy tunnel experimental section of the Qinghua Garden on the Beijing-Zhangjiakou Railway. Donna et al. (2016), based on the energy tunnel section of Line 1 of the Turin Metro in Italy, studied the stress and strain performance of shield tunnel segments during heat exchange through on-site experiments. The experimental results showed that the stress and strain generated in the lining during heat exchange are within an adjustable range.

The research results mentioned above demonstrate that the impact of heat exchangers on tunnel structures during heat exchange in energy tunnels is relatively small. However, different types of heat exchangers, due to their different installation forms, may have varying mechanical impacts on tunnel structures during heat exchange.

There are significant differences in structure, physical performance, and construction methods between capillary heat exchangers and traditional ground heat exchangers. Therefore, one cannot simply infer the heat transfer characteristics and the structural-mechanical impact on tunnel structures of one type of heat exchanger based on the other. This study analyzed the thermal-structural coupling characteristics of prefabricated capillary heat exchangers in energy shield tunnel segments during heat exchange based on a specific engineering project in Qingdao city.

2. MODEL ESTABLISHMENT

The principle of the SSHPS based on shield tunnel, as shown in Figure 1. The system utilizes capillary tubes laid inside the shield tunnel segments as front-end heat exchangers, with each shield tunnel segment serving as a heat exchange unit. Utilizing the reverse Carnot cycle of the heat pump unit, in cooling season, heat is extracted from buildings and transferred and released into the subway tunnel to achieve cooling. In heating season, waste heat or residual heat is extracted from the subway tunnel and used for heating buildings to maintain comfortable temperatures.

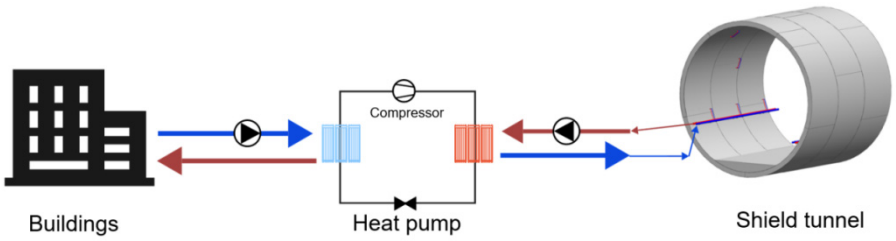

Figure 1: Principle of the SSHPS

2.1. Geometric model

The shield tunnel segments are arranged in a 1+2+3 combination, comprising the crown segment (F), adjacent segment (L1, L2), and standard segment (B1, B2, B3). CHE are prefabricated only in the two adjacent segments (L1, L2) and the two standard segments (B1, B3) adjacent to the adjacent segments. Therefore, each ring of the shield tunnel contains two capillary loops on the left and right sides. The main capillary pipes inside the segments are arranged along the circumferential direction of the tunnel, while the branch pipes are arranged using a non-uniform distribution method.

In this study, the spacing between individual capillary branch pipes inside the tunnel segment is 5mm, and the spacing between each group of capillary branch pipes is 44mm. The diameter of the CHE branch pipes is 4.3mm with a wall thickness of 0.85mm. The diameter of the main branch pipe is 18mm with a wall thickness of 2mm. The way of laying CHE in segments is shown in Figure 2.

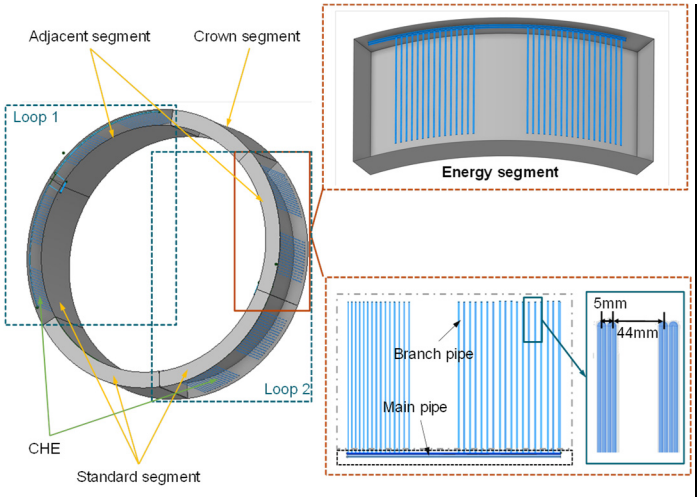

Figure 2: CHE layout

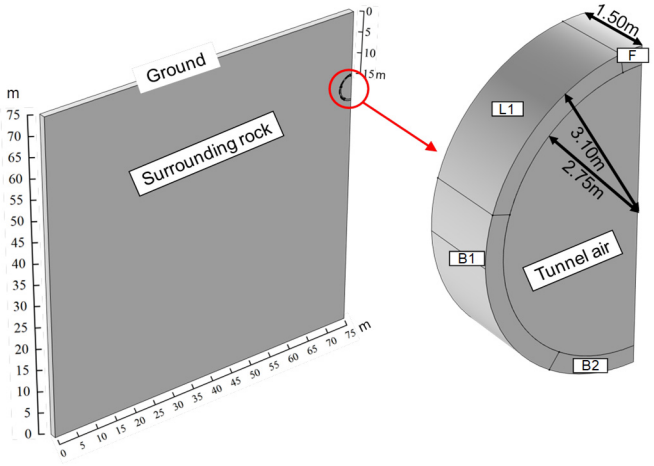

Figure 3: Geometric model of energy tunnel

Referring to the demonstration project, the inner diameter of the shield tunnel segment is 5.5 meters, the outer diameter is 6.2 meters, and the height is 1.5 meters. The depth of the tunnel top is approximately 15 meters. The shield tunnel segments in the actual engineering project are assembled in a staggered manner. To reduce computational complexity, this simulation only considers the case where the top block is located directly above the tunnel. Following the principle of symmetry, only half of the tunnel segment is considered for calculation, comprising half of the crown segment (F), half of the standard segment (B2), as well as the adjacent segment (L1) and the standard segment (B1). To minimize the influence of boundary conditions on the model calculation results, the length and width of the surrounding rock are both set to 75 meters. The geometric model is established as shown in Figure 3.

2.2. Numerical model

This study utilized the COMSOL Multiphysics finite element software to simulate the heat exchange performance of the CHE and the structural-mechanical response of the shield tunnel segments under typical cooling season and heating season design conditions in energy tunnels. The simulations were conducted using the Turbulent Flow Module, Heat Transfer in Solids and Fluids Module, Non-Isothermal Pipe Flow Module, Solid Mechanics Module, and Beam Module, respectively, to model the airflow in the tunnel, heat transfer between tunnel air, tunnel segments, and surrounding rock, heat transfer between CHE and tunnel segments, and tunnel stress.

The research focus of this study is the analysis of the thermal-structural coupling characteristics of tunnel segments in energy shield tunnels. It explores the heat transfer characteristics of the prefabricated CHE and the structural-mechanical response of shield tunnel segments during CHE operation, involving several complex coupled physical field problems. To simplify calculations, the following assumptions are made:

（1）Surrounding rock, lining, and CHE have constant material properties and are isotropic.
（2）Contact thermal resistance is neglected.
（3）The influence of groundwater flow on the heat transfer process is disregarded.
（4）During system operation, the fluid inside the CHE and the airflow in the tunnel remain constant.
（5）The surrounding rock is simplified as a linear elastic model.
（6）Gravity is ignored.

Based on the aforementioned simplifications, the numerical model obtained in this study is as follows:

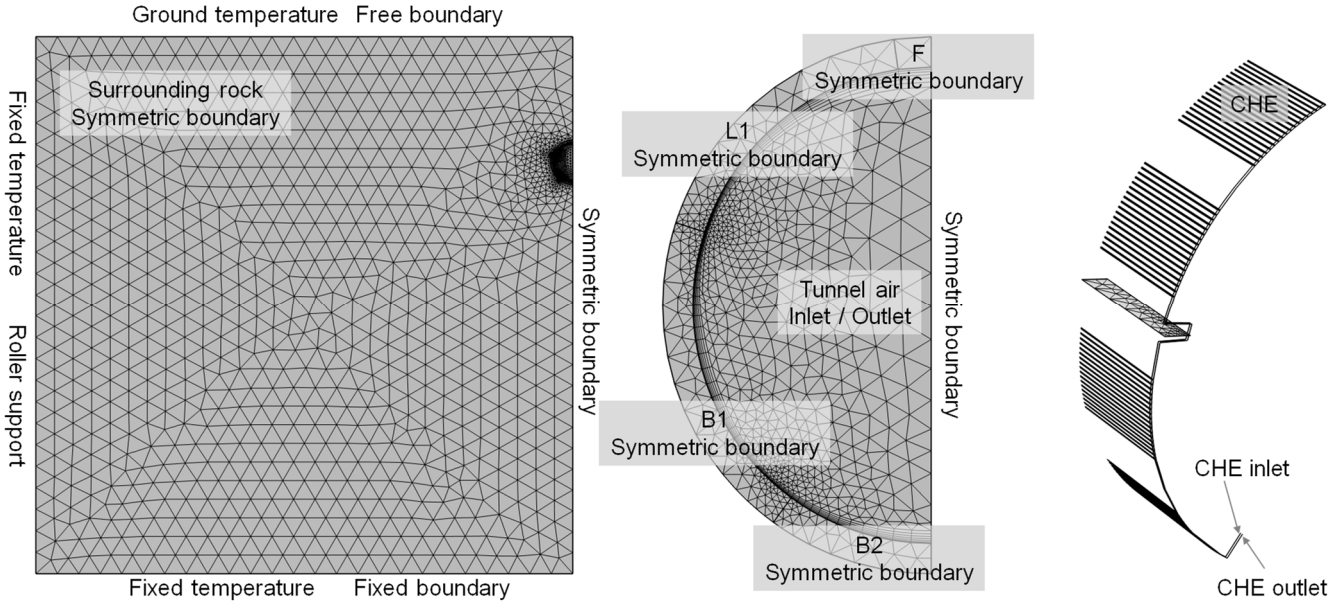

Figure 4: Geometric model of energy tunnel

As shown in figure 4, the numerical model is configured as follows:

- The left boundary is set as roller support, allowing only vertical displacement and restricting horizontal displacement.
- The top boundary is set as the ground (free boundary).
- The bottom boundary is set as a fixed boundary, allowing for settlement of the surrounding rock.
- For shield tunnels with more than 4 segments, the "Code for Design of Metro" recommends using a beam-spring model for calculation (11.6 Code for design of metro. GB50157-2013). This method considers that the bolted joints of circular lining structures can bear certain forces, and the deformation of the joints is linearly related to internal forces, treating the joints as elastic hinges.

Hence, in the simulation process, linear elastic solid elements are used to simulate the segments and surrounding rock, while springs are used to simulate the joints. The axial spring constant and tangential spring constant of the joints are set to 3×10^7kN/m and 1×10^6kN/m (Zhu and Tao, 1998), respectively. Other physical property parameters of the model were set with reference to an actual engineering project in Qingdao, as shown in Table 1.

Table1: Physical property parameters of the model

	Density (kg/m^3)	Thermal conductivity (W/m)	Specific heat capacity (J/(kg*K))	Young modulus (Gpa)	Poisson's ratio (1)	Thermal expansivity (1/K)
Segment	2700	5.56	935	33.5	0.2	0.00001
Surrounding rock	2800	3.49	920	0.009	0.3	0.000007
CHE pipe	900	0.24	2000			
Water	998.2	0.60	4182		—	
Air	1.225	0.0242	1006.43			

2.3. Boundary conditions

The variation of wind speed inside the tunnel mainly consists of three different stages: when trains pass through, no trains are passing, and during nighttime ventilation. When trains pass through, the maximum wind speed inside the tunnel is approximately 6.5 m/s. After the train passes through, the air inside the tunnel becomes relatively stable, with the wind speed is about 0.5 m/s (Zhang et al, 2020). Since the simulation method used in this study is steady-state calculation, the tunnel wind speed is set to the average speed during train operation, which is approximately 4.61 m/s (Ji, Wu and Hu, 2023). According to measurements from the demonstration project, the average tunnel temperatures during the cooling and heating seasons are approximately 28°C and 12°C, respectively.

Based on previous research findings, the recommended flow velocity for the capillary heat exchanger is 0.08 m/s (Gao, 2015). According to Section 29.3.3 of the "Practical Handbook of Heating, Ventilation, and Air Conditioning Design (Second Edition)" (Volume II), the design temperatures for the outlet of the ground source heat pump unit on the source side are 6°C and 35°C for the heating and cooling modes respectively (Lu, 2008). Therefore, the inlet water temperature of the CHE is set to 6°C and 35°C for the heating and cooling seasons respectively.

For the simulation of heating season and cooling season, the ground temperature is taken as the average outdoor temperature during the heating and cooling seasons in Qingdao, which are approximately 2.8°C and 25°C, respectively. The fixed temperature is taken as the annual average outdoor temperature in Qingdao, which is 14.6°C (Ji et al, 2022).

The values of boundary conditions are summarized in Table 2.

Table 2: boundary conditions

	Cooling season	Heating season
Wind speed (m/s)	4.61	
Tunnel air inlet temperature (℃)	28	12
Tunnel air outlet relative pressure (Pa)	0	
CHE flow velocity (m/s)	0.08	
CHE inlet temperature (℃)	35	6
CHE outlet relative pressure (Pa)	0	
Ground temperature (℃)	25	2.8
Fixed temperature (℃)	14.6	

3. INITIAL CONDITIONS

The initial conditions of the model are set to represent the scenario where the capillary heat exchanger is not operational. Only the temperature field formed by the heat exchange between the subway tunnel, the ground, and the subway air is considered, as shown in Figure 5.

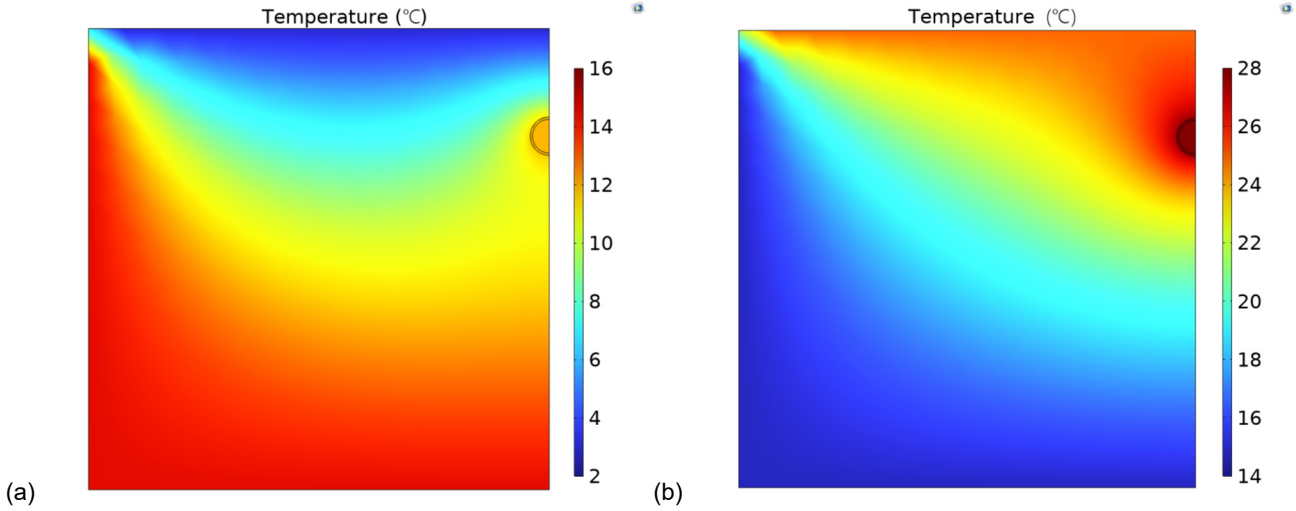

Figure 5: Initial temperature field of the model: (a) cooling season; (b) heating season

As shown in figure 5, The initial temperature field of the model is non-uniform.

The initial displacement field of the model is set to 0m.

4. RESULT AND DISCUSSION

Based on the simulation settings described above and using a steady-state calculation method, the thermal performance of the prefabricated capillary heat exchanger in the energy tunnel and the structural-mechanical response of the tunnel under design conditions were simulated in heating season and cooling season.

4.1. Heat-transfer characteristic

Figure 6 is the temperature field after the operation of the CHE.

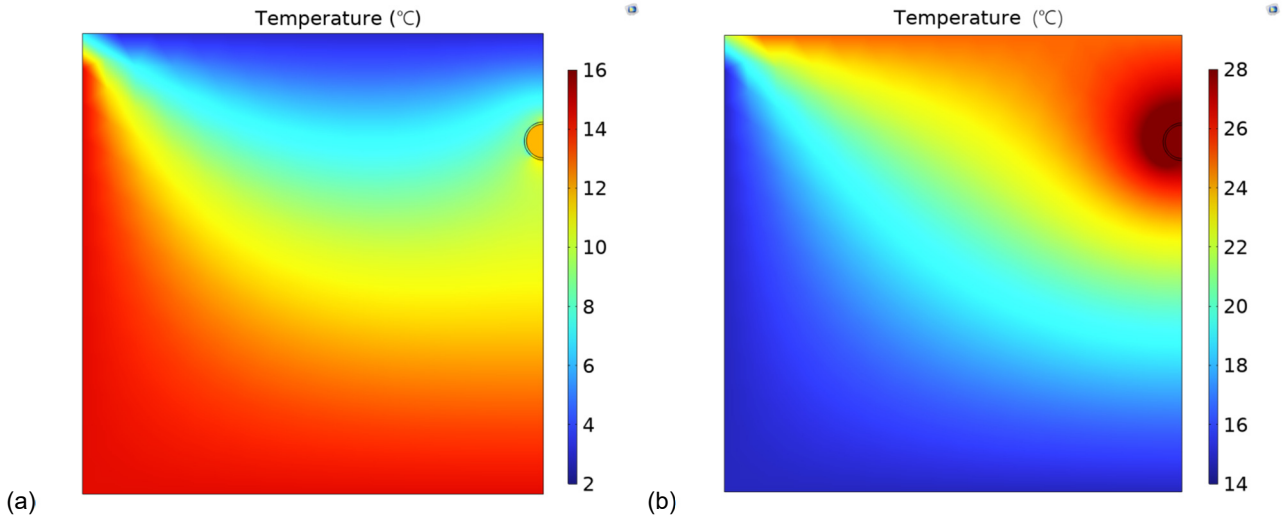

Figure 6: Temperature field of the model after the operation of CHE: (a) cooling season; (b) heating season

Compared to the initial temperature field, there are significant changes in the temperature field around the tunnel. In heating season, the temperature of the surrounding rock slightly decreases, while in cooling season, the temperature of the surrounding rock around the tunnel significantly increases. The reason for this phenomenon is that in heating season, the inlet temperature of the capillary heat exchanger is 6°C, while the initial temperature around the tunnel is approximately 11°C, resulting in a temperature difference of 5°C. In cooling season, the inlet temperature of the capillary heat exchanger is 35°C, while the initial temperature around the tunnel is approximately 27°C, resulting in a temperature difference of 8°C. The temperature difference in heating season is significantly smaller than in cooling season, leading to smaller changes in the temperature field.

CHE temperature distribution is shown in Figure 7.

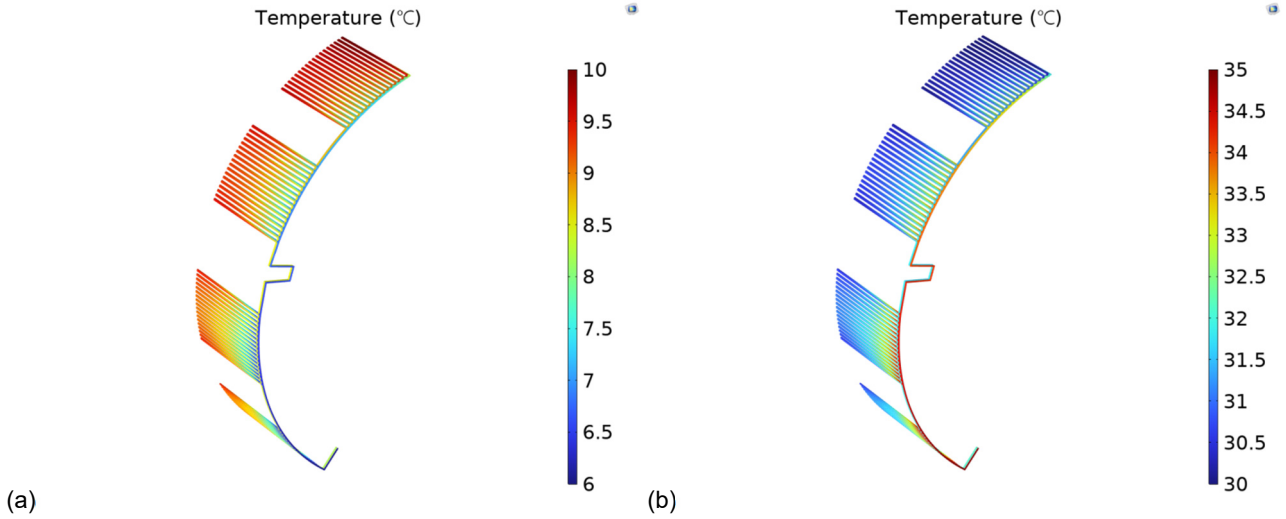

Figure 7: Temperature field of the CHE: (a) cooling season; (b) heating season

In heating season, with the inlet temperature of the CHE set to 6°C, the computed outlet temperature of CHE is approximately 8.22°C. The temperature difference between inlet and outlet under steady-state design conditions is about 2.22°C. The average temperature of the fluid inside the CHE pipe is 8.74°C.

In cooling season, with the inlet temperature of CHE set to 35°C, the computed outlet temperature of CHE is approximately 32.12°C. The temperature difference between inlet and outlet under steady-state design conditions is about 2.88°C. The average temperature of the fluid inside the CHE pipe is 31.40°C.

As shown in Figure 8, overall, in both heating season and cooling season, the temperature distribution of CHE exhibits higher variations at the sides and lower variations in the middle. This is because the CHE on the sides are less influenced by the heat exchange from other CHE, resulting in higher heat transfer efficiency. The heat transfer rates of CHE are illustrated in Figure 8.

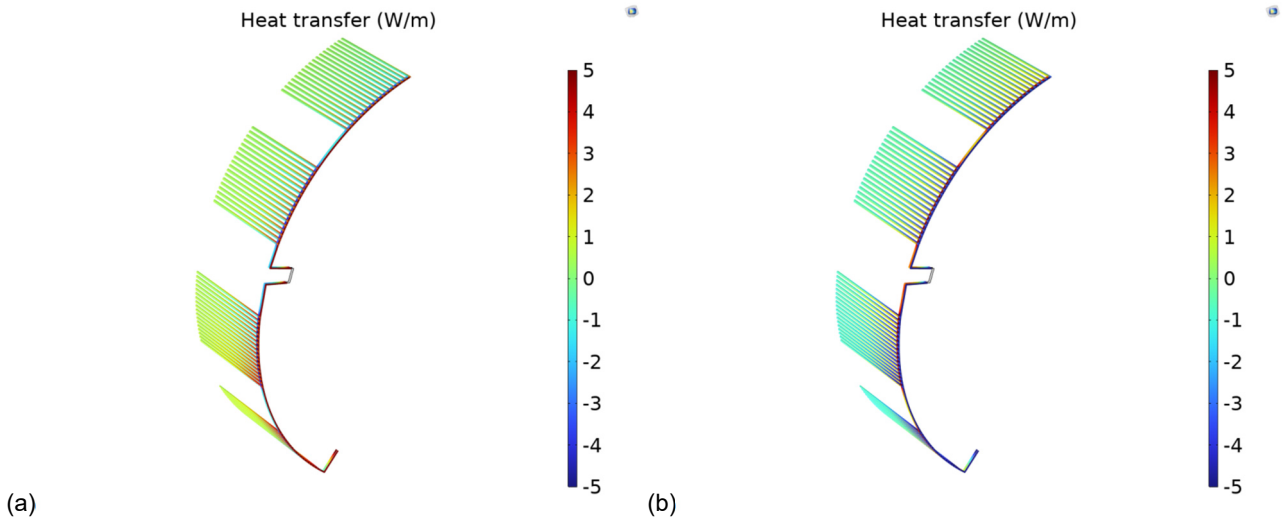

Figure 8: Heat transfer in CHE: (a) cooling season; (b) heating season

The distribution trend of heat transfer in the CHE in heating season and cooling season follows the same trend as the temperature distribution. The main pipe of the supply water pipe, where the CHE inlet is located, exhibits the highest heat transfer, but the main pipe and branch pipes of the return water pipe, where the CHE outlet is located, have opposite heat conduction directions (in heating season, the branch pipes absorb heat while the return water pipes release heat; in cooling season, the branch pipes release heat while the return water pipes absorb heat).

In heating season, the average heat transfer per unit pipe length is 0.60 W/m, and the total heat transfer of CHE in the entire numerical model is 233.14 W. Thus, it can be calculated that the heat transfer per loop of the prefabricated capillary heat exchanger in the shield energy tunnel is approximately 466.28 W. In cooling season, the average heat transfer per unit pipe length is 0.77 W/m, and the total heat transfer of CHE in the entire numerical model is 300.81 W. Therefore, the heat transfer per loop of the prefabricated capillary heat exchanger in the shield energy tunnel is approximately 601.62 W.

The projected area of CHE in the model is calculated to be approximately 4.74 m². Therefore, it can be inferred that the unit area heat transfer of the prefabricated capillary heat exchanger in the shield energy tunnel in heating season and cooling season is 49.19 W/m² and 63.46 W/m², respectively.

4.2. Structural characteristic

In this study, the steady-state calculation method was employed to simulate the structural mechanical response of the subway tunnel after the operation of the CHE, primarily focusing on the thermal stress of the shield tunnel segments.

Equivalent stress (Von Mises stress) is a stress representation method proposed by Austrian engineer Von Mises. It predicts the deformation behavior of materials under complex stress states by considering the stress components in different directions. Although equivalent stress cannot directly assess the failure risk of materials, it provides an overview of stress distribution. Its calculation method is as follows:

Equation 1: Calculation method of equivalent stress.

$$\sigma_{eq} = \sqrt{{}^{1}/_{2}\left((\sigma_1 - \sigma_2)^2 + (\sigma_2 - \sigma_3)^2 + (\sigma_3 - \sigma_1)^2\right)}$$

Where:

- σ_{eq} = Equivalent stress (MPa)
- σ_1 = Major principal stress (MPa)
- σ_2 = Secondary principal stress (MPa)
- σ_3 = Third principal stress (MPa)

The equivalent stress distribution in heating season and cooling season is shown in Figure 9.

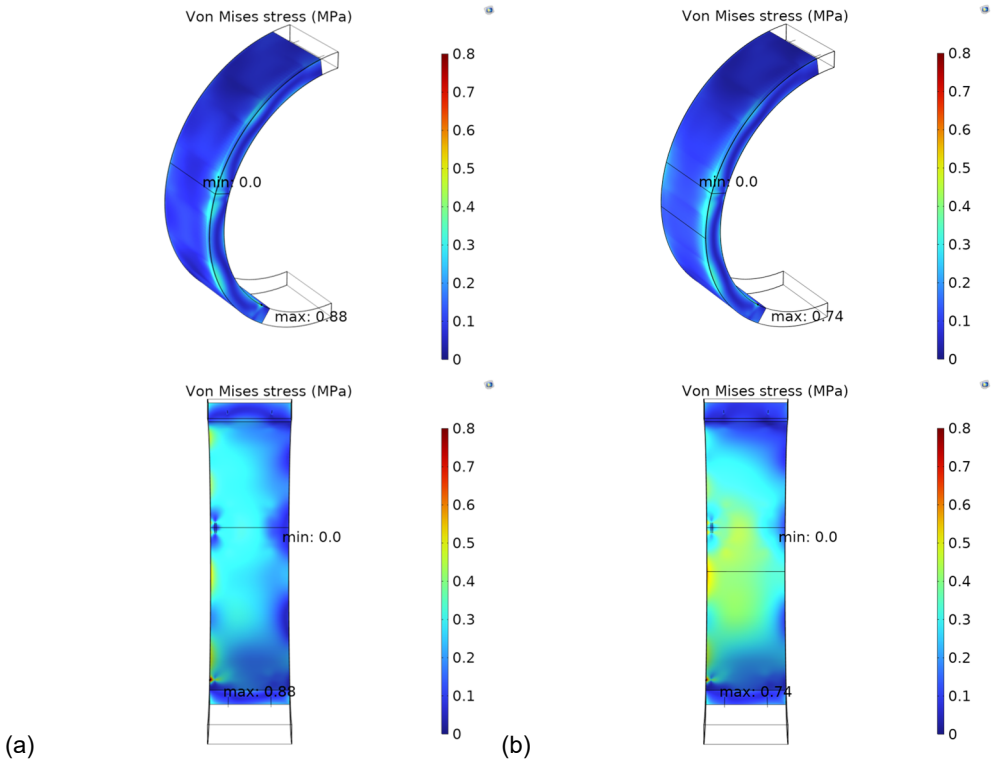

Figure 9: Equivalent stress distribution of segment: (a) cooling season; (b) heating season

The maximum equivalent stresses in heating season and cooling season both occur at the CHE inlet, with values of 0.74MPa and 0.88MPa respectively. The secondary maximum values are located beneath the waist of the inner side of the tunnel segments. Therefore, during construction, it is important to avoid overlapping stresses at the CHE inlet with other stress concentrations.

In cooling season, with a CHE inlet temperature of 35°C and an inlet flow velocity of 0.08 m/s, the principal stress calculations are as follows:

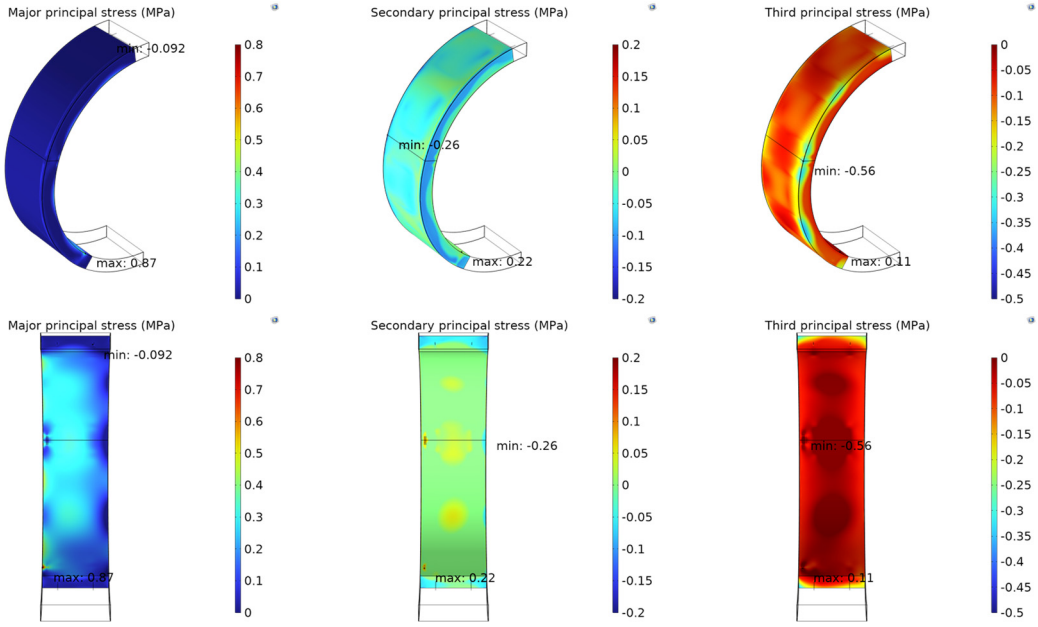

Figure 10: Principal of segment in cooling season

During cooling season, the tunnel segments are heated, causing an increase in temperature. As shown in Figure 10, the tunnel segments experience overall tensile stresses. However, the deformation of the segments is constrained by the surrounding rock, resulting in compressive stresses on the outer arc face and tensile stresses on the inner arc face. The maximum compressive stress occurs at the waist of the outer arc face, measuring 0.56 MPa, while the maximum tensile stress is observed at the CHE inlet, reaching 0.87 MPa.

In heating season, with a CHE inlet temperature of 6°C and an inlet flow velocity of 0.08 m/s, the principal stress calculations are as follows:

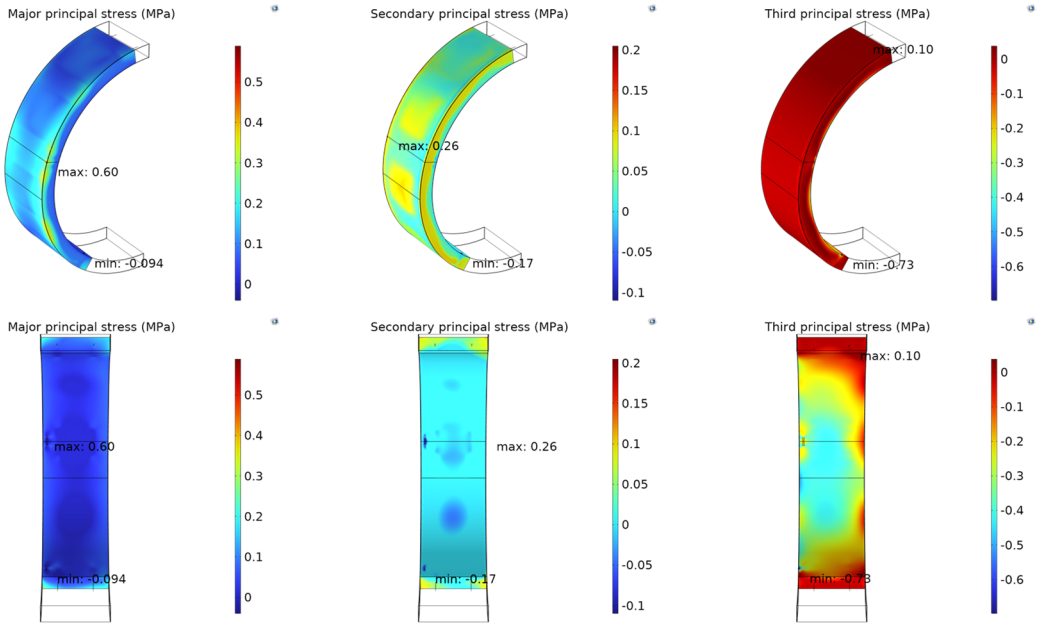

Figure 11: Principal of segment in heating season

The tunnel segments are cooled in heating season, resulting in a decrease in temperature. As depicted in Figure 11, the tunnel segments experience overall compression. Similarly to heating season, the deformation of the segments is restricted by the surrounding rock, leading to tensile stresses on the outer arc face and compressive stresses on the inner arc face. The maximum tensile stress occurs at the waist of the outer arc face, measuring 0.60 MPa, while the maximum compressive stress is observed at the CHE inlet, reaching 0.73 MPa.

The distribution of equivalent stresses in the tunnel segments during heating season and cooling season is similar, with the maximum equivalent stress occurring at the CHE inlet. This could be attributed to the significant temperature variation and temperature gradient at this location. It is recommended to position the CHE inlet at the midpoint of the tunnel segment to avoid stress concentration. The deformation status of the tunnel segments in heating season and cooling season is opposite, with the outer side experiencing tensile stresses and the inner side experiencing compressive stresses in heating season. Conversely, in cooling season, the outer side experiences compressive stresses, and the inner side experiences tensile stresses. The maximum compressive stresses are 0.56 MPa and 0.73 MPa in cooling season and heating season respectively, which are far below the compressive limit of C50 concrete (50 MPa). The maximum tensile stresses are 0.87 MPa and 0.60 MPa in cooling season and heating season respectively, representing 33% and 23% of the axial tensile strength of C50 concrete (2.64 MPa). It is advisable to avoid the overlap of these positions with the locations of maximum tensile stresses during the construction process.

5. CONCLUSION

This study, based on COMSOL Multiphysics finite element analysis software, utilized steady-state numerical calculation methods to simulate the thermal-structure coupling characteristics of the prefabricated capillary heat exchanger (CHE) in the energy shield tunnel under design conditions, leading to the following conclusions:

（1）Under the design conditions of the heat pump unit, the system exhibits good heat transfer performance. When the inlet temperatures are 35°C in cooling season and 6°C in heating season, the outlet water temperatures of CHE are approximately 32.12°C and 8.22°C, respectively. Each ring of the energy shield tunnel can provide heat transfer rates of 601.62W and 466.28W in heating season and cooling season, respectively, with heat transfer efficiencies reaching 63.46W/m² and 49.19W/m².
（2）In cooling season, CHE operation causes the segments to stretching, while in heating season, it leads to contract of the segments. However, the deformation of the segments is influenced by the surrounding rock of the tunnel, resulting in compression on the outer arc surface and tension on the inner arc surface in cooling season, with the opposite occurring in heating season.
（3）Due to CHE operation, the maximum tensile and compressive stresses generated in cooling season are 0.87MPa and 0.56MPa, respectively, while in heating season, they are 0.60MPa and 0.73MPa, respectively. The compressive stresses are far below the compression limit of C50 concrete, while the tensile stresses account for 33% and 23% of the axial tensile strength, respectively.
（4）The distribution of equivalent stresses reveals that the maximum stress points on the segments are located at the CHE inlet in both cooling season and heating season, reaching 0.88 MPa and 0.74 MPa, respectively.

Therefore, the prefabricated CHE in the energy shield tunnel demonstrates good heat transfer performance, with minimal impact on the tunnel segment. However, caution should be exercised to avoid complete overlap between the inlet and outlet of CHE on the segments and the positions of maximum tensile stress occurring during the tunnel construction process.

6. REFERENCES

National Bureau of Statistics, (2022) 'China Statistical Yearbook'. Beijing shu tong dian zi chu ban she. (In Chinese)

Jiang, Y. Hu, S. and Zhang Y., et al. (2022) 'China building energy efficiency annual development research report'. (In Chinese)

Geothermal energy information. (2023) Qian, Q.H: establish and improve the mechanism of shallow geothermal energy application. Available at: https://mp.weixin.qq.com/s/r9odhwxjE340mrIfddnxjA (Accessed: 15 August 2023).

Brandl, H. (2006). 'Energy foundations and other thermo-active ground structures'. Géotechnique, 56(2), pp.81-122.

Adam, D., and Markiewicz, R. (2009) 'Energy from earth-coupled structures, foundations, tunnels and sewers'. Géotechnique, 59(3), pp.229-236.

Wang, H.Y. Hu, S.T. and Chang Z. et al. (2014) The invention relates to a capillary soil source heat pump system applied to a subway tunnel. (2014-03-05). CN103615841A.

Xia, C.C. Yang, Y. Zhang, G.Z. and Zou, Y.C. (2014) 'The internal source heat pump heat exchange tube and tunnel structure interact'. Journal of Tongji University (Natural Science Edition), (1), pp.51-57. (In Chinese)

Yang, Y. Xia, C.C. and Zhu, J.L. (2014) 'Study on temperature stress induced by heat exchange tube of tunnel ground source heat pump'. Journal of Central South University: Natural Science Edition, 45(11), pp.3970-3976. (In Chinese)

Zhu, Z.N. (2020) 'Analysis of heat transfer, stress and construction problems of energy shield tunnel'. (Master's thesis, Tsinghua University).

Di Donna, A. and Barla, M. (2016) 'The role of ground conditions on energy tunnels' heat exchange'. Environmental geotechnics, 3(4), pp.214-224.

Ministry of Construction of the People's Republic of China. (2013) 'GB 50157-2013 Code for design of metro'. Beijing: China Building Industry Press.

Ministry of Construction of the People's Republic of China. (2005) 'GB 50366-2005 Technical code for ground-source heat pump system'. Beijing: China Building Industry Press.

Zhu, H.H. and Tao, L.B. (1998) A beam-spring system model for stress analysis of shield tunnel lining structures. Journal of Rock and Soil Mechanics, 19(2), pp.26-32. (In Chinese)

Zhang, Y. Zhang, Q. Bi, H.Q. and Wang, J.Y. (2020) 'Experimental study on wind speed and its variation in metro piston duct'. Refrigeration and air conditioning (Sichuan), 34(04), pp. 463-467. (In Chinese)

Ji, Y.M, Wu, W.Z. and Hu, S.T. (2023) 'Long-term performance of a front-end capillary heat exchanger for a metro source heat pump system'. Applied Energy, 335, p.120772.

Gao, H. (2015) Research on Heat Transfer Characteristics of Capillary Heat exchangers in Subway Tunnel (Doctoral dissertation, Qingdao: Qingdao University of Technology).

Lu Y.Q. (2008) 'Practical heating and air conditioning design manual. second ed'. Beijing: China Construction Industry Press. (In Chinese).

Ji, Y.M. Wu, W.Z. Qi, H.Y. Wang, W.Q and Hu, S.T. (2022) 'Heat transfer performance analysis of front-end capillary heat exchanger of a subway source heat pump system'. Energy, 246, p.123424.